Quantitative Mass Spectrometry Reveals Food Intake-Induced Neuropeptide Level Changes in Rat Brain: Functional Assessment of Selected Neuropeptides as Feeding Regulators*[S]

Hui Ye‡§¶¶, Jingxin Wang¶ ¶¶, Zichuan Tian‖, Fengfei Ma§, James Dowell§, Quentin Bremer, Gaoyuan Lu‡, Brian Baldo¶**§§, and Lingjun Li§¶‖‡‡§§**

Endogenous neuropeptides are important signaling molecules that function as regulators of food intake and body weight. Previous work has shown that neuropeptide gene expression levels in a forebrain reward site, the nucleus accumbens (NAc), were changed by feeding. To directly monitor feeding-induced changes in neuropeptide expression levels within the NAc, we employed a combination of cryostat dissection, heat stabilization, neuropeptide extraction and label-free quantitative neuropeptidomics via a liquid chromatography-high resolution mass spectrometry platform. Using this methodology, we described the first neuropeptidome in NAc and discovered that feeding caused the expression level changes of multiple neuropeptides derived from different precursors, especially proSAAS-derived peptides such as Big LEN, PEN and little SAAS. We further investigated the regulatory functions of these neuropeptides derived from the ProSAAS family by performing an intra-NAc microinjection experiment using the identified ProSAAS neuropeptides, 'Big-LEN′ and 'PEN′. Big LEN significantly increased rats' food and water intake, whereas both big LEN and PEN affected other behaviors including locomotion, drinking and grooming. In addition, we quantified the feeding-induced changes of peptides from hippocampus, hypothalamus and striatum to reveal the neuropeptide interplay among different anatomical regions. In summary, our study demonstrated neuropeptidomic changes in response to food intake in the rat NAc and other key brain regions. Importantly, the microinfusion of ProSAAS peptides into NAc revealed that they are behaviorally active in this brain site, suggesting the potential use of these peptides as therapeutics for eating disorders. ***Molecular & Cellular Proteomics 16: 10.1074/mcp.RA117.000057, 1922–1937, 2017.***

Neuropeptides represent the largest and most diverse class of cell-to-cell signaling molecules that modulate neurotransmission. These short amino acid chains regulate a wide range of processes such as stress, pain, addiction, memory, circadian rhythm, reproduction, and food intake (1–4). Quantitative description of the expression levels of these peptide neuromodulators can enhance understanding of the mechanisms underlying neuropeptide action, and can facilitate the discovery of novel neuropeptides that may represent effective drug-development targets in multiple neurological and psychiatric illnesses (2, 5).

Neuropeptide actions have been studied extensively about their involvement in motivational disorders, including drug addiction, obesity, and eating disorders. Interestingly, several studies have suggested significant overlap in peptide-based mechanisms between drug addiction and the hedonistic aspects of feeding (6–9). Much of this work has focused on the actions of opioid peptides, which is understandable given the significant abuse liability of the opiate class of drugs (10–16). A theory has emerged stating that opioids regulate motivational function by enhancing the primary rewarding properties of calorie-dense food and drugs of abuse, in part by modifying neural activity in the nucleus accumbens (NAc)[1], a forebrain

From the ‡State Key Laboratory of Natural Medicines, Key Lab of Drug Metabolism and Pharmacokinetics, China Pharmaceutical University, Tongjiaxiang #24, Nanjing 21009, China; §School of Pharmacy, University of Wisconsin-Madison, 777 Highland Avenue, Madison, Wisconsin 53705; ¶Neuroscience Training Program, University of Wisconsin-Madison, 1111 Highland Avenue, Madison, Wisconsin 53705; ‖Department of Chemistry, University of Wisconsin-Madison, 1101 University Avenue, Madison, Wisconsin 53706; **Department of Psychiatry, University of Wisconsin-Madison, 6001 Research Park Boulevard, Madison, Wisconsin 53719; ‡‡School of Life Sciences, Tianjin University, No. 92 Weijin Road, Nankai District, Tianjin 300072, China

Received August 9, 2017
Published, MCP Papers in Press, September 1, 2017, DOI 10.1074/mcp.RA117.000057
Author contributions: H.Y., J.W., B.B., and L.L. designed research; H.Y., J.W., F.M., J.A.D., Q.B., B.B., and L.L. performed research; H.Y., J.W., Z.T., F.M., G.L., B.B., and L.L. analyzed data; H.Y., J.W., Z.T., B.B., and L.L. wrote the paper.

[1] The abbreviations used are: NAc, nucleus accumbens; HRAM, high resolution accurate mass; PTM, post-translational modification; DS, dorsal striatum; hippo, hippocampus; HT, hypothalamus; CAN, acetonitrile; MeOH, methanol; DDA, data-dependent acquisition; IT, injection times; HCD, higher-energy collisional dissociation; NCE,

site that crucially regulates the effects of both natural and drug rewards. For example, direct intra-NAc infusion of opioid peptides (primarily those acting at the mu-opioid receptor, such as endorphins and enkephalins) markedly increases food intake. Indeed, this is among the largest drug-induced feeding effects elicited from anywhere in the brain, with rats consuming up to 400% of their normal intake of food (17). Feeding-associated behavioral states also markedly influence the striatal expression of enkephalin genes. Will and coworkers found that expression of preproenkephalin mRNA in the NAc was significantly upregulated in a food-anticipation state relative to a satiety state (18), suggesting that transcriptional activation of the striatal enkephalin system is linked to the motivational drive to eat. Nevertheless, mRNA expression studies can only reveal transcript-level changes that do not always reflect changes in peptide levels. Mass spectrometry (MS)-based analyses can provide this missing information, thereby validating and extending the inferences gleaned from gene expression studies.

MS-based analyses can also address a common limitation of neuropharmacological and gene-expression studies of peptide neuromodulation; namely, that these approaches typically examine only one peptide or peptide family at a time (19–22). The regulation of food intake is, however, an intricate process that takes place via a complex neural network involving coregulation of multiple neuropeptides from different peptide families. Currently, relatively little information is available regarding how diverse neuropeptide families change comprehensively in response to feeding motivational states. Furthermore, cross-talk and interplay of a multitude of feeding-responsive neuropeptides, both within a specific brain region and across different brain regions, has not been examined previously.

To obtain a more comprehensive analysis of feeding-associated peptide changes in the NAc and other sites, we employed a combination of cryostat dissection, neuropeptide extraction and label-free quantitative neuropeptidomics using liquid chromatography coupled with high resolution accurate mass Orbitrap mass spectrometer. This approach enables simultaneous detection of many neuropeptides from specific brain regions of interest in a high-throughput manner, and avoids several pitfalls of older methods. Historically, neuropeptides have been predominantly studied employing radioimmunoassay, immunohistochemistry, and Edman degradation (20). These techniques continue to be important, but recent advances in MS have provided a new and powerful analytical platform to study neuropeptides (21, 22). MS-based neuropeptidomics can identify and quantifying many neuropeptides simultaneously, yielding higher throughput and specificity, whereas immuno-based approaches suffer from relatively low throughput and possible cross-reactivity among different members of the same peptide family. Furthermore, these older methods could not accurately identify and characterize the neuropeptides with additional post-translational modifications (PTMs) such as acetylation, C-terminal amidation, and N-terminal pyro-glutamic acid.

MS-based neuropeptidomic analysis of mammalian tissue samples does, however, suffer from nonspecific protein degradation. This process can produce peptide contamination peaks that can mask the signals of the less abundant endogenous neuropeptides (23, 24). Previous attempts to curtail postmortem protein degradation have employed a number of methods, including the use of transgenic mice lacking carboxypeptidase E activity (25), processing samples in a boiling buffer (26), focused microwave irradiation for animal sacrifice (27), and rapid postsacrificial microwave irradiation (28) Microwave irradiation heat deactivates endogenous proteases and arrests postmortem protein degradation, resulting in a clean neuropeptide sample for MS analysis. Alternatively, a Denator™ apparatus has been developed to rapidly and focally heat individual tissue samples, and has been shown to minimize nonspecific protein degradation that might convert endogenous neuropeptides to other forms, thereby greatly enhancing accurate peptide identification and quantitation (29, 30). Consequently, our lab has employed a neuropeptidomics workflow combining snap freezing, cryostat dissection, and snap heat stabilization using Denator. We therefore anticipate that the neuropeptides described in this study represent mostly bioactive mature neuropeptides and intermediate cleavage products with potential biological functions.

The goal of the present study was to directly interrogate feeding-induced changes in endogenous peptides, using the MS-based neuropeptidomic approach described above, in four feeding-modulatory brain regions: NAc, dorsal striatum (DS), hippocampus (hippo) and hypothalamus (HT) (11, 31, 32). Notably, such peptidomic changes in response to food intake have never been characterized in the NAc region previously. We analyzed tissue punches from these brain regions in two groups of rats. In the "unfed" group, food was withheld during a 2-hour period spanning the change from the light to dark cycle, a period in which rats (which are nocturnal) normally exhibit intense feeding responses and are primed to eat because of circadian factors. In the "fed" group, rats had access to food during this time, and completed a meal. This protocol mirrors the methodology used in prior studies of feeding-responsive striatal enkephalin gene expression (18). Our peptidomic approach enabled the investigation of two interrelated questions: (1) Can MS-based peptide quantification methods reveal the feeding-related peptide gene-expres-

normalized collision energy; BCA, bicinchoninic acid; AGC, automatic gain control; UPLC, ultraperformance liquid chromatography; CCK, cholecystokinin; proTRH, prothyrotropin-releasing hormone; PACAP, pituitary adenylate cyclase-activating polypeptide; CARTPT, cocaine- and amphetamine-regulated transcript protein; VGF, neurosecretory protein VGF; PENK, proenkephalin; PDYN, prodynorphin; POMC, proopiomelanocortin; PENK A, proenkephalin-A; PENK B, Proenkephalin-B; NPY, neuropeptide Y; VIP, vasoactive intestinal peptide; PC 1/3, prohormone convertase 1/3; icv, intracerebroventricular.

sion changes reported in previous literature, and (2) What are the coordinated changes across diverse peptide families and brain regions in fed *versus* unfed behavioral states? Finally, we explored the physiological relevance of novel peptides uncovered in the NAc, by synthesizing the peptides, infusing them directly into the NAc, and monitoring ethologically relevant ingestive and exploratory-like behaviors.

EXPERIMENTAL PROCEDURES

Experimental Design and Statistical Rationale—The objective of this study is to perform comprehensive characterization of the neuropeptide changes because of food intake in four different rat brain regions from 12 fed and unfed adult male Sprague-Dawley rats by a label-free neuropeptidomics approach. 24 rats were all sacrificed 2 h after the experimental manipulation (*i.e.* food given or food withheld). Rat brains were immediately dissected following decapitation and the DS, hippo, HT and NAc regions were isolated as tissue punches, followed by rapid heating via Denator™ to minimize postmortem degradation. Four punches were pooled for each aliquot of NAc and hippo ($n = 3$ for each group), three punches were pooled for an aliquot of HT ($n = 4$ for each group), and two punches were pooled for each aliquot of DS as an aliquot ($n = 6$ for each group) to minimize individual variation and increase the amount of neuropeptides contained in samples. Each punch was sampled from an individual animal. The sample aliquots were then processed independently, and analyzed with LC-MS/MS on an Orbitrap platform. The MS/MS data were searched against a home-built rat neuropeptide database in PEAKS Studio for peptide identification. Relative expression level changes of the identified peptides were calculated by comparing the peak areas calculated based on extracted ion chromatograms (XIC) of each peptide. Statistical significance in peptide abundance levels between the unfed and fed groups was determined by Student's *t* test.

Following the differential analysis of neuropeptidome, we chose several ProSAAS peptides that changed significantly on feeding by performing microinjection experiments on rat NAc. Stainless-steel guide cannulae were implanted above the NAc shell for 10 Sprague-Dawley rats. After recovery from surgery, rats received intra-NAc infusions and were placed into a behavior-observation procedure to appraise the behavioral changes of rats injected with ProSAAS-derived peptides. To explore changes in behavioral patterns over time, the first hour continuous recording of bouts and duration of each behavior was divided into 12 × 5 min time-bins. These data were subjected to two-way ANOVA (treatment X time), with repeated measures for the time factor, and posthoc analyses were carried out using Tukey's test. $p < 0.05$ was considered as statistically significant for all experiments.

Chemicals and Reagents—Optima grade formic acid, acetonitrile (ACN), water, and methanol (MeOH) were purchased from Fisher Scientific (Pittsburgh, PA). All other chemicals were obtained from Sigma-Aldrich (St. Louis, MO).

Animals—Adult male Sprague-Dawley rats (total $n = 24$, Harlan Sprague-Dawley, Indianapolis, IN) weighing 300–400 g were maintained in a temperature- and humidity-controlled animal colony on a 12:12-h light-dark cycle (lights off at 18:00). All subjects were naive and were allowed a minimum of a week adaptation followed by 2 days of daily handling before the beginning of the experiment. Subjects had free access to normal laboratory chow (24% protein, 4% fat) and drinking water was available *ad libitum*. On the day of the experiment, at 17:00, food (chow) was removed from half of the subjects, while a measured amount of food was given to the other subjects (18 g/cage). The rats were then killed at 19:00, 2 h after food was given. The time point was chosen based on the previous mRNA experiment performed in the lab (18). All experimental procedures were in accordance with protocols approved by the University of Wisconsin Institutional Animal Care and Use Committee.

Sample Preparation—

Animal Sacrifice and Cryostat Dissection—Rats were anesthetized with isoflurane and then sacrificed by decapitation. The brain was then rapidly removed (<90 s) and snap frozen in 2-methylbutane cooled by dry ice. The frozen brain was then sectioned in 300 μm thick slices on a cryostat from Leica (Wetzlar, Germany) with a compartment temperature of −15 °C. The regions corresponding to DS, hippo, HT, and NAc were removed with a 2 mm micro-punch and stored in 1.5 ml tubes at −80 °C until extraction (see Fig. 1).

Heat Stabilization and Tissue Extraction—Tissue punches (20–30 mg per rat) were removed from −80 °C and immediately processed by Denator Stabilizor T1 tissue stabilization device (Gothenburg, Sweden) for heat stabilization. Tissue punches were placed in a Stabilizor cartridge as a pooled aliquot. The pooled aliquots were then inserted into the device, and stabilized using the fresh preserve tissue function. The stabilization process involved uniformly heating the tissue to 95 °C for 30–45 s (depending on the tissue thickness). After stabilization, tissue was removed from the cartridge, placed in the appropriate extraction solvent, and stored at −80 °C until needed.

The processed tissues were then extracted into ice-cold acidified methanol (90:10:1, MeOH: water: acetic acid) as previously described (33). The samples were then homogenized manually with a glass-glass Dounce homogenizer from Wheaton (Millville, NJ). The homogenized sample was then spun at 20,000 × *g* for 20 min at 4 °C to remove the insoluble pellet. Protein concentration of the pellet was determined for each sample using bicinchoninic acid (BCA) assay from Pierce (Rockford, IL) and used to adjust the differences in the neuropeptide levels contained in different sample aliquots. The adjusted supernatant was decanted and then dried in a vacuum centrifuge. Extracts were resuspended in 20 μl 0.1% formic acid aqueous solution by vortexing and brief sonication. Subsequently, the reconstituted samples were purified and concentrated by C_{18} ZipTip (Millipore, Billerica, MA). Briefly, the C_{18} ZipTip was first wetted using ACN and then pre-equilibrated for sample binding with 0.1% formic acid in water. Subsequently, the tissue extract was loaded on the C_{18} ZipTip. After being rinsed three times with 0.1% formic acid in water, the sample was eluted with 5 μl of ACN/water/formic acid solution (50:49.9:0.1; v/v/vol). Next, the eluent was dried and resuspended in 10 μl of 0.1% formic acid in water and subjected to future LC-MS/MS analysis.

Liquid Chromatography Coupled to Mass Spectrometry—Peptide extracts from each brain sample aliquot were analyzed separately. Peptide samples were dissolved in 0.1% FA before analysis. A Waters nanoAcquity ultraperformance liquid chromatography (UPLC) (Waters Corp., Milford, MA) was coupled to a Thermo Q-Exactive Orbitrap mass spectrometer (Thermo Fisher Scientific, San Jose, CA) for LC-MS/MS analysis. Chromatographic separations were performed on a Waters BEH 130 Å C18 reversed-phase capillary column (150 mm × 75 μm, 1.7 μm). The mobile phases used were: mobile phase A consisted of water with 0.1% FA, and mobile phase B was composed of ACN with 0.1% FA. Samples were injected and loaded onto the Waters NanoACQ 2G-V/M Sym C_{18} (20 mm ×180 μm, 5 μm) using 100% A at a flow rate of 5 μl/min for 1 min. Then the peptides were separated using a solvent gradient of 0–10% B over 0.5 min and then 10–30% B over 70 min at a flow rate of 300 nL/min. Data-dependent acquisition (DDA) parameters recorded MS scans in profile mode from *m/z* 380–1500 at a resolution of 35,000. Automatic gain control (AGC) targets of 1×10^6 and maximum injection times (IT) of 100 ms were set. The 15 most intense precursor ions were selected for MS^2 higher-energy collisional dissociation (HCD) fragmentation with an isolation window of 2 Da and dynamic exclusion set at 40 s. An AGC

target of 1×10^5 and a maximum IT of 150 ms was selected for tandem mass acquisition. The tandem MS spectra were acquired at a resolution of 17,500 in profile mode, with normalized collision energy (NCE) set at 27, and a fixed lower mass at *m/z* 110.

Label-free Quantitation of Neuropeptides—

Neuropeptide Identification—All the raw LC-MS/MS data were imported to PEAKS Studio 7.0 (BSI, Waterloo, Ontario, Canada) for peptide identification. Data processing procedures, including peak centroiding and charge deconvolution, were conducted to refine the raw data. To perform a neuropeptide search using the PEAKS DB algorithm, the enzyme was specified as none. The peptide mass tolerance was set at 10 ppm and the MS/MS mass tolerance was set at 20 ppm. The variable modifications were set to include amidation (C-terminal), acetylation (protein N-terminal), and Gln->pyro-Glu (N-terminal). No enzyme specificity was required. The database search was conducted using an in-house built neuropeptide database and a Swiss-prot database (7710 entries for rats). The cutoff of false discovery rate (FDR) for peptide identification was set below 1%. A decoy fusion method was employed by PEAKS for FDR calculation. It concatenates the decoy and target sequences of the same protein together as a "fused" sequence instead of directly concatenating the target and decoy databases together, and the FDR is estimated by dividing (# Decoy Hits) by (# target hits) (34). Peptide spectrum matches (PSMs) with a −10logP value cutoff of 30 in PEAKS were considered for further manual inspection. All the spectra used for identification assigned by PEAKS were subsequently manually checked. For PTM assignment, a minimum of three consecutive b or y ions must be present in the MS/MS spectra.

Neuropeptide Quantitation—Relative expression level changes were calculated for each identified peptide pair by comparing the peaks areas calculated using extracted ion chromatograms (XIC). Such differential analysis was conducted using PEAKS Studio 7.0. The acquired LC/MS/MS data were first aligned by the software. Using one of the samples for each region as a reference, the peak areas of each identified peptides were then extracted after TIC normalization, and the differential analysis was conducted on the unfed and fed samples region by region. A *t* test was performed between unfed and fed groups, and any pair at $p < 0.05$ was considered as statistically significant. The parameters used were as follows: *m/z* range: 300–2000; retention time window = 5 min; ion *m/z* width = 10 ppm; retention time range: 5–80 min. A *t* test between unfed and fed groups was performed for identified peptides, and any pair at $p < 0.05$ was considered as statistically significant. Moreover, the MS S/N ratio of all significantly changed peptides was larger than 50. The mass spectrometric data have been deposited to the MassIVE system and accessible from *ftp://ztian29@massive.ucsd.edu* with the username of "ztian29" and "Ratfeeding" as the password.

Microinjection to the Nucleus Accumbens Using Neuropeptides Exhibiting Significant Changes Across Feeding States—

Subjects—Ten Sprague-Dawley rats (Harlan; Madison, WI) weighted 300–400 g when arriving at the laboratory were housed in clear cages in a temperature and light-controlled vivarium (lights on from 0700 to 1900, 12:12 h light-dark cycle). Food and water were available *ad libitum* and all experiments were conducted between 1000–1600 h. The rats were handled daily to reduce stress except the period during recovery from surgery. Facilities and procedures followed the guidelines of animal use and care from the National Institutes of Health, and were approved by the Institutional Animal Care and Use Committee of the University of Wisconsin.

Surgical Procedure—Rats were anesthetized with isoflurane while undergoing stereotaxic surgery. Stainless-steel cannulae (10-mm long; 25 gauge) were implanted bilaterally 2.5 mm above the NAc shell (coordinates from bregma with toothbar at +5 mm above interaural zero: + 3.2 anteroposterior (AP); ± 1.0 lateromedial (LM); −5.2 dorsoventral (DV). The guide cannulae were cemented with dental acrylic (New Truliner, Skokie, IL) and skull screws (Plastics One, Roanoke, VA). Stylet wires (10.1 mm long, 0.008 in. diameter) were placed in the guide cannulae to prevent blockage. Intramuscular penicillin (0.3 ml of a 300,000 U/ml suspension; Phoenix Pharmaceuticals, St. Joseph, MO) and Meloxicam were given to the animals after surgery. Animals were placed in a warm recovery cage and returned to their original cages on awakening. Animals were given 10 days of daily health checks before behavioral testing commenced.

Experimental Design—Before all experiments, rats were placed into the testing cages to be habituated for one hour on three sequential days to minimize stress. Two-hour free-feeding test sessions were conducted in the clear polycarbonate cages (9.5 in. width × 17 in. length × 8 in. height), which were identical to their home cages except for a wire grid floor. After recovery from surgery, animals were acclimated to the microinfusion procedures with preliminary sham and saline injections. Subsequently, drug testing commenced.

Rats had free access to laboratory chow and water before drug injection. On the testing day, rats ($n = 10$) received intra-NAc shell infusions (3, 10 μg/0.5 μl PEN, 3, 10 μg/0.5 μl big LEN) and were placed into a behavior-observation procedure (discussed below). For each drug, doses were administered in accordance with within-subject Latin square designs, with 2–3 interim drug-free days separating the drug-infusion days. After finishing the infusion of big LEN and PEN at two dosages in a counterbalanced order, all the rats ($n = 10$) were given another saline injection to rebaseline them. After rebaseline, all the rats ($n = 10$) were given an injection of little-SAAS (10 μg/0.5 μl) to determine its effect, because the quantitative results of little-SAAS showed smaller fold-changes compared with PEN or big LEN. Finally, DAMGO (0.25 μg/0.5 μl) was given to all the rats ($n = 10$) to compare the behavioral changes of ProSAAS-derived peptides to the known effects of an opioid receptor agonist.

Behavioral Observation Procedure—After 1-hour habituation sessions were carried out for three sequential days (described above), the rats were injected with their specific treatment respectively. Immediately after infusion, rats were placed into the wire-bottom polycarbonate cages (described above) with premeasured laboratory chow pellets placed on the floor of the testing cages, while premeasured water was available in overhead bottles. Meanwhile, they were videotaped with a digital camcorder for 2 h. Spontaneous motor and ingestive behaviors were scored off-line by an experimenter blind to treatment, using an event-recorder program interfaced with a PC-based computer (35). The following parameters were scored: locomotion (crossing over the cage center), feeding, drinking, rearing, grooming. The total duration (in seconds) and frequency of each behavior were scored except locomotion, for which only frequency was scored. The first hour test period was divided into 12 × 5 min time-bins and the effects of treatment was determined as a function of time during this session. Finally, total food and water ingested (corrected for spillage) were measured for each test session.

Microinfusion Procedures and Drugs—Intracerebral microinfusions were performed in accordance with previously published procedures (36). The injectors (12.5 mm) extended 2.5 mm beyond the guide cannulae. Big-LEN, PEN and little-SAAS were purchased from Phoenix Pharmaceuticals (Burlingame, CA). DAMGO (μ-opioid agonist) was obtained from Sigma-Aldrich (St. Louis, MO). The dosage-range of big-LEN, PEN and little-SAAS used here were like that applied in previous studies (37). All drugs were dissolved and diluted with fresh sterile 0.9% saline immediately before the infusions.

Statistical Analyses—Within-subject factorial ANOVAs were applied for data analyses as required by the experimental designs. Data with significant changes in ANOVAs were subjected to posthoc comparisons among means using the Tukey-Kramer method. To explore the changes of behavioral patterns over time, the first hour continuous

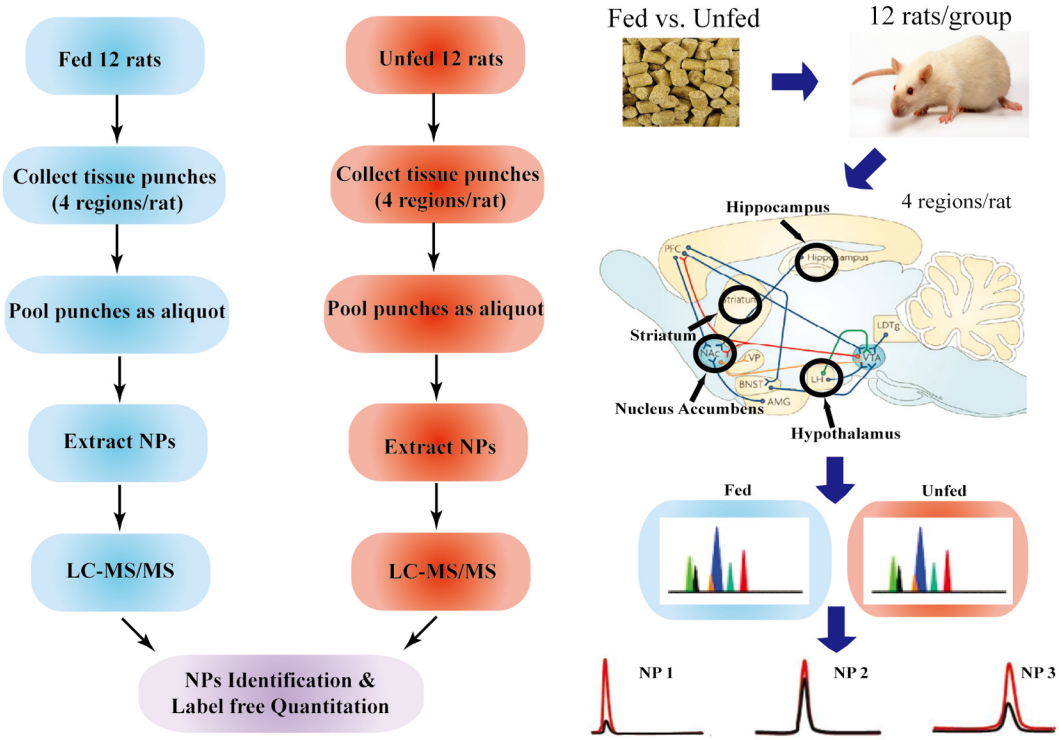

FIG. 1. **The experimental paradigm of the quantitative mass spectrometry we employed to investigate the neuropeptide level changes in response to food intake.** Rats fed on a regular diet or starved were all sacrificed 2.5 h after the feeding time. Rat brains were immediately dissected following decapitation and the dorsal striatum, hippocampus, hypothalamus and nucleus accumbens regions were collected as tissue punches, followed by rapid heating by Denator™ to minimize postmortem degradation. The tissue samples were pooled as an aliquot to minimize individual variation and increase the amount of neuropeptides contained in samples. Four punches were pooled for NAc and hippo, three punches were pooled for HT and two punches were pooled for DS as an aliquot. The sample aliquots were then processed individually, and the endogenous neuropeptides were analyzed by an Orbitrap LC-MS/MS. The high accuracy MS and MS/MS data yielded by Orbitrap were searched against database for identification, whereas peak areas calculated using the extracted ion chromatograms of each identified peptide are employed for relative quantitation. The locations of the tissue punches we collected are shown on a sagittal slice of the rat brain.

recording of bouts and duration of each behavior was divided into 12 × 5 min time-bins. These data were subjected to two-way ANOVA (treatment X time), with repeated measures for the time factor, and posthoc analyses were carried out using Tukey's test. $p < 0.05$ was considered as statistically significant for all experiments.

RESULTS

In this study, we aimed to perform comprehensive characterization of the neuropeptide changes because of food intake in four different rat brain regions by comparing neuropeptidomic profiles of 12 fed and unfed rats (Fig. 1). Rats were sacrificed 2 h after the experimental manipulation (*i.e.* food given or food withheld). Rat brains were immediately dissected following decapitation and the DS, hippo, HT and NAc regions were collected as tissue punches, followed by rapid heating via Denator™ to minimize postmortem degradation. The four brain regions were selected because of their involvement in food intake or reward-related neuropeptide signaling. The respective tissue samples were pooled as an aliquot to minimize individual variation and increase the amount of neuropeptides contained in samples. The sample aliquots were then processed individually ($n = 3$ for NAc and hippo, $n = 4$ for HT, $n = 6$ for DS), and the endogenous neuropeptides were analyzed by an Orbitrap LC-MS/MS. The high accuracy MS and MS/MS data yielded by Orbitrap were searched against a home-built database, enabling comprehensive identification and quantification of neuropeptides from different brain regions induced by food-intake. Among neuropeptides that displayed significant changes in response to food intake (13, 19, 21, 37, 49, 50), we chose to investigate the putative regulatory roles of several ProSAAS peptides that changed significantly on feeding by performing microinjection experiments on rat NAc in the current study.

Identification of Neuropeptides from Rat Dorsal Striatum, Hippocampus, Hypothalamus, and Nucleus Accumbens—To understand the underlying mechanism of neuropeptides' impact on food intake, an initial step is to comprehensively identify the neuropeptides present in the targeted rat brain regions. The high resolution, high accuracy MS and MS/MS information acquired from the peptides following nanoLC separation enabled by the Orbitrap ensures high confidence peptide identification. HCD MS/MS fragmentation in conjunction with charge deconvolution and deisotoping of the MS/MS

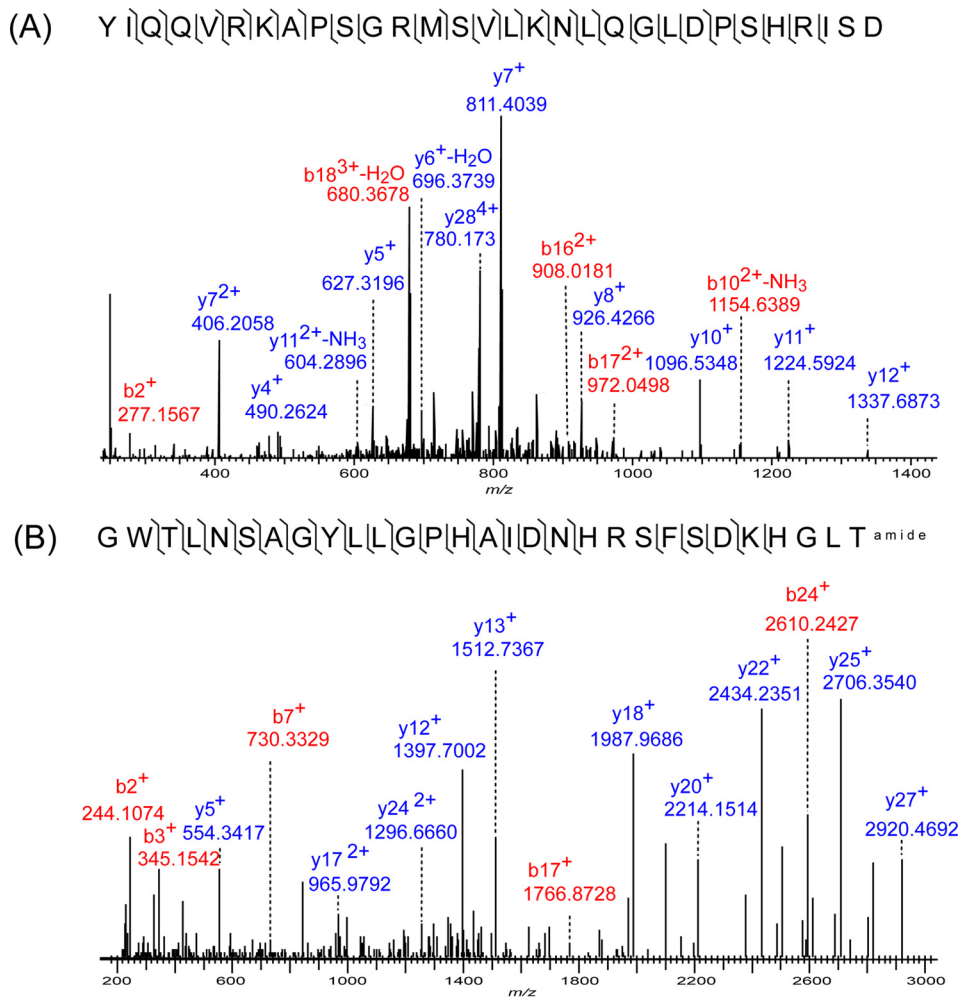

FIG. 2. **High resolution mass spectrometry enabled identification of highly and moderately charged neuropeptides with high confidence.** *A*, The MS/MS spectra of a 5+ charged peptide ions detected at *m/z* 679.569 identified as YIQQVRKAPSGRMSVLKNLQGLDP-SHRISD from the neuropeptide precursor cholecystokinin. *B*, MS/MS identification of a moderately-charged 3+ ion at *m/z* 1055.197 characterized as GWTLNSAGYLLGPHAIDNHRSFSDKHGLTamide (galanin).

spectra permit the interpretation of the relatively highly-charged neuropeptides. Fig. 2*A* shows the MS/MS spectra of a 5+ charged peptide ions detected at *m/z* 679.569. Using a stringent searching criterion, mass tolerance for precursor ions at 10 ppm and product ions at 20 ppm, the precursor ion in Fig. 2*A* was identified as YIQQVRKAPSGRMSVLKN-LQGLDPSHRISD from the neuropeptide precursor cholecystokinin (CCK) with high confidence (a −10logP score of 145.65, in which −10logP denotes the *p* value of database search). Besides a few highly charged peptide ions, most of the neuropeptides identified were 2+, 3+ charged. Fig. 2*B* illustrates the identification of a moderately-charged 3+ ion at *m/z* 1055.197 characterized as galanin derived from the galanin peptides family (GWTLNSAGYLLGPHAIDNHRSFSDKH-GLTamide,-10logP = 126.09) with a mass error of −2.2 ppm (Table I). All the LC-MS/MS data was searched against a home-built database that originated from the reviewed Swiss-prot database of *Rattus norvegicus* and then filtered to retain precursors that contain signal peptide sequences. With this database, we reported the identification of 635 endogenous peptides derived from 37 precursors from the four brain regions in total. A complete summary of all the identified peptides and their presence in the four regions is provided in, supplemental Table S1, and the MS/MS spectra of peptides that have been detected from only one biological replicate are summarized in supplemental Fig. S1.

With the peptidomes of DS, Hippo, HT and NAc being characterized, we then analyzed the overlap of peptides among the four regions in Fig. 3*A*. HT was found to be the region containing the highest number of endogenous peptides (585 peptides). It also contained the largest number of unique peptides (167 peptides, 26.3% of peptidome) that are non-overlapped with other regions. These peptides were mainly derived from precursors including secretogranin 2, ProSAAS, secretogranin 1, neurosecretory protein VGF (VGF), Prothyrotropin-releasing hormone (proTRH), Proenkephalin-A

TABLE I

*Representative neuropeptides and prohormone-derived peptides identified from rat nucleus accumbens and their corresponding changes induced by food intake. (−0.98) denotes C-terminal amidation. Asterisk denotes significantly changed peptides in response to food intake. Fed/unfed ratio represents the relative level changes of peptides upon feeding. * denotes $p < 0.05$, ** denotes $p < 0.01$, and *** denotes $p < 0.005$*

Gene	Precursor	Accession	Name	Peptide	PTM	-10lgP	*m/z*	z	Mass	ppm	Fed/unfed Ratio	*p* value
PCSK1	ProSAAS	Q9QXU9	truncated little SAAS	R.SLSAASAPLAETSTPL.R*		99.00	758.3997	2	1514.7827	1.4	0.45	0.0483
PCSK1	ProSAAS	Q9QXU9	big LEN	R.LENSSPQAPARRLLPP*		84.23	873.4865	2	1744.9584	0	0.42	0.0311
PCSK1	ProSAAS	Q9QXU9	little SAAS	R.SLSAASAPLAETSTPLRL.R***		125.24	892.9910	2	1783.9679	−0.3	0.56	0.0003
PCSK1	ProSAAS	Q9QXU9	PEN	R.AVDQDLGPEVPPENVLGALLRV.K*		133.03	767.7530	3	2300.2375	0.3	0.7	0.0297
PCSK1	ProSAAS	Q9QXU9	Big SAAS	S.ARPVKEPRSLSAASAPLAETSTPLRL.R		120.49	680.3869	4	2717.5188	−0.1	0.71	0.1062
Cartpt	Cocaine- and amphetamine−regulated transcript protein	P49192		R.APGAVLQIEALQEVLKKLKS.K***		107.84	534.5759	4	2134.2725	1	1.46	0.0041
Mch	Pro-MCH	P14200	MCH	R.EIGDEENSAKFPI(−0.98).G	C-termamidation	104.33	724.3575	2	1446.6990	1	n.s.	
gal	Galanin peptides	P10683	galanin	R.GWTLNSAGYLLGPHAIDNHRSFSDKHGLT(−0.98).G**	C-termamidation	112.13	633.5222	5	3162.5747	−0.1	0.6	0.0067
Scg2	Secretogranin-2	P10362		R.IPAGSLKNEDTPNRQYLDEDMLLKVLE.Y*		112.21	776.1509	4	3100.5750	−0.2	0.65	0.0194
Chga	Chromogranin-A	P10354		R.WSRMDQLAKELT.A*		89.04	739.3776	2	1476.7395	0.7	1.63	0.0369
Tac3	Tachykinin-3	P08435	Neurokinin B	R.DMHDFFVGLM(−0.98).G	C-termamidation	86.97	605.7739	2	1209.5311	1.7	n.s.	
Npy	Pro-neuropeptide Y	P07808	C-flanking peptide of NPY	R.SSPETLISDLLMRESTENAPRTRLEDPSMW		80.38	866.1731	4	3460.6602	0.9	n.s.	
Npy	Pro-neuropeptide Y	P07808	Neuropeptide Y	G.YPSKPDNPGEDAPAEDMARYYSALRHYINLITRQRY(−0.98).G	C-termamidation	122.48	712.5214	6	4269.0811	0.8	n.s.	
Tac1	Protachykinin-1	P06767	Neurokinin A	R.HKTDSFVGLM(−0.98).G	C-termamidation	76.02	567.2933	2	1132.5699	1.8	n.s.	
Tac1	Protachykinin-1	P06767	substance P	R.RPKPQQFFGLM(−0.98).G	C-termamidation	79.55	674.3711	2	1346.7281	−0.4	n.s.	
Tac1	Protachykinin-1	P06767	truncated neuropeptide K	R.DADSSIEKQVALLKALYGHGQISHK.R*		116.99	677.8652	4	2707.4292	0.9	1.51	0.0314
Penk	Proenkephalin-A	P04094	PENK(114–133)	K.MDELYPVEPEEEANGGEILA.K		78.76	1102.9993	2	2203.9829	0.5	n.s.	

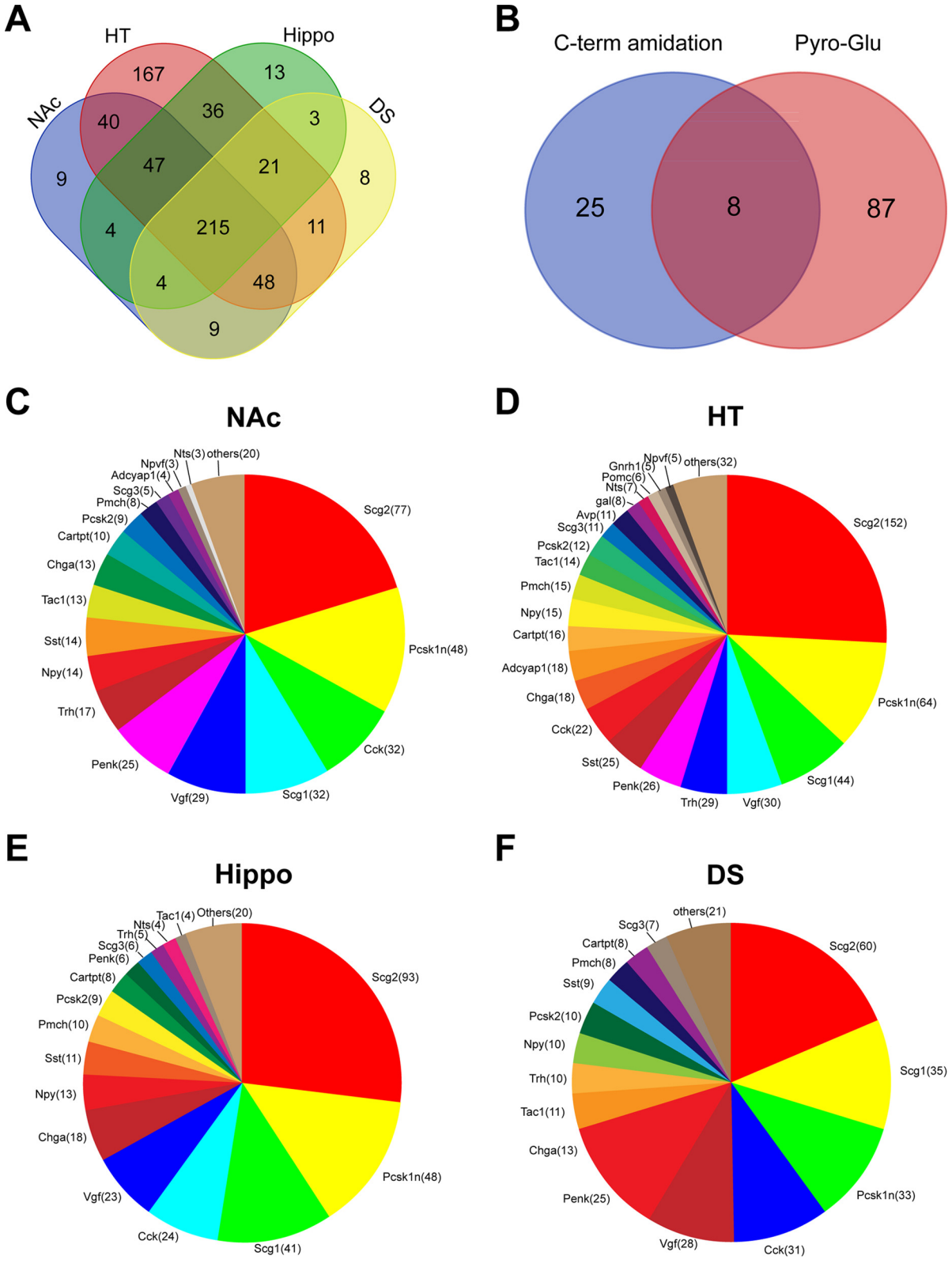

FIG. 3. **Summary of the endogenous peptides identified from rat brain.** *A*, Overlap of unique peptides identified from hypothalamus (HT), hippocampus (hippo), nucleus accumbens (NAc), and dorsal striatum (DS). *B*, Overlap of peptides carrying pyro-Glu modification and C-terminal amidation. Distribution of the number of peptides per protein (shown in parenthesis) for the precursors yielding more than 5 peptides from NAc (*C*), HT (*D*), hippo (*E*) and DS (*F*).

(PENK), somatostatin, and CCK. In contrast, DS, Hippo and NAc only had 8 (1.3%), 13 (2.0%) and 9 (1.4%) nonoverlapping peptides, respectively. The peptides exclusively detected in the DS regions were mainly from CCK and proenkephalin-A, whereas the hippocampus-unique peptides were mostly derived from secretogranin-2 and chromogranin-A. Additionally, the CCK, secretogranin-2 and ProSAAS-derived peptides consist of the NAc peptidome was nonoverlapping with the other regions. This observation is consistent with a previous report that compared the neuropeptidome of HT with DS, which also detected significantly more peptides from the HT region compared with the striatum region (38).

Notably, 215 peptides (33.5% of the entire characterized peptidome) were shared among all four brain areas. The overlapping peptides were mainly derived from the well-characterized neuropeptide precursors such as secretogranin-2, ProSAAS, secretogranin-1, CCK, VGF, proTRH, neuropeptide Y (NPY), somatostatin, CARTPT and proenkephalin-A. Such a large portion of shared peptides might reveal the conservative roles the detected peptides are involved in among different neuroanatomical regions. A detailed analysis of the peptidome from different regions is summarized in supplemental Table S2.

Out of the identified 642 peptides (including PTMs), 120 peptides carry one or multiple PTMs as summarized in Fig. 3*B*. Ninety-five peptides (79.2% of the modified peptides) carry a pyro-glutamate produced by cyclization of the N-terminal glutamine, whereas 33 peptides (27.5% of the modified peptides) with PTM possess a C-terminal amidation. Interestingly, both two modifications could convert the inactive versions of incompletely-processed peptides into active and mature forms (38). For example, the peptides RPKPQQFFGLM and HKTDSFVGLM cannot be processed to the active neuropeptides substance P and neurokinin A (which modulate numerous processes including immune responses, nociception, and addiction) without C-terminal amidation.

Fig. 3*C*–3*F* shows the distribution of variant neuropeptide families identified from each brain regions. As expected, HT consists of the most variant neuropeptide precursors, containing 22 precursors that each possesses more than five unique peptides. These families include secretogranin-2, ProSAAS, secretogranin-1, VGF, proTRH, proenkephalin-A, somatostatin, and CCK. Of all identified endogenous peptides, galanin, MCH and NPY are all known to regulate food intake (detailed information see Table I). Besides the well-known mature neuropeptides, many peptides identified here are truncated forms or longer forms of these neuropeptides. These immature forms are normally intermediate neuropeptide products produced during neuropeptide maturation process by processing enzymes such as carboxypeptidases or extracellular peptidases. The truncated peptides are likely products resulting from postmortem degradation, which is also suggested by the detection of several peptides from stathmin, a postmortem protein marker (supplemental Table S3). Nevertheless, the mature peptides are often observed at much higher signal intensities than the fragments that represent either processing intermediate or postmortem degradation, such as substance P (RPKPQQFFGLMamide, peak area at a E+09 scale) *versus* its nonamidated form (RPKPQQFFGLM, peak area at a E+07 scale), which reflected a minor impact of such degradation on the characterized neuropeptidome in this study (supplemental Table S4).

DS, Hippo, and NAc possessed 15, 14, and 15 families of precursors that yielded more than 5 unique peptides, showing less diversity of neuropeptide composition compared with the HT region. This accorded with the results we showed in Fig. 3*A*, probably because of HT's largest sample area and greater heterogeneity than other regions (38). It is worth noticing that the second largest number of peptides found in the NAc were derived from the precursor ProSAAS. ProSAAS has several known physiological functions, including inhibiting the activities of prohormone convertase (25). Moreover, ProSAAS deletion leads to the decrease of body mass and overexpression of ProSAAS results in obesity (39). Our current investigation of whether the ProSAAS-derived peptides were changed because of food intake could help unravel the postulated functions of ProSAAS peptides in regulating food intake, body weight, and energy homeostasis. In addition to ProSAAS, proenkephalin-A is another primary component of all the identified peptides in NAc. This observation is in accord with the fact that enkephalins are highly abundant in the NAc, where they modulate behaviorally relevant neural function (40, 41).

Label-free Quantitation of Neuropeptides Induced by Feeding—To perform a robust yet accurate label-free quantitative experiment, we randomized the samples and analyzed the pooled tissue samples in three replicates for each region. PEAKS studio was employed for postacquisition processing of the acquired LC-MS/MS data (34). The software extracted the peak areas for identified peptides and subsequently revealed the peptides with altered expression levels by quantifying the peak area ratio for each peptide between the fed *versus* unfed group. Supplemental Table S4 summarizes the relative expression level changes of the identified peptides from the four brain areas, including DS, HT, hippo, and NAc. Although most of the peptides identified in this study showed no significant differences between the fed and unfed samples because of high variations among samples and limited sample size within the pool, some peptides were found to change significantly following food intake. A summary of these peptides is shown in Table I, which not only includes the bioactive neuropeptides known to be involved in feeding regulation but also linker peptides that have not been reported previously. Therefore, this comprehensive quantitative analysis of rat neuropeptidome greatly expands our knowledge of peptides associated with food intake.

Notably, we observed several ProSAAS-derived neuropeptides that changed significantly in response to food intake. Specifically, ProSAAS represents a neuropeptide family that

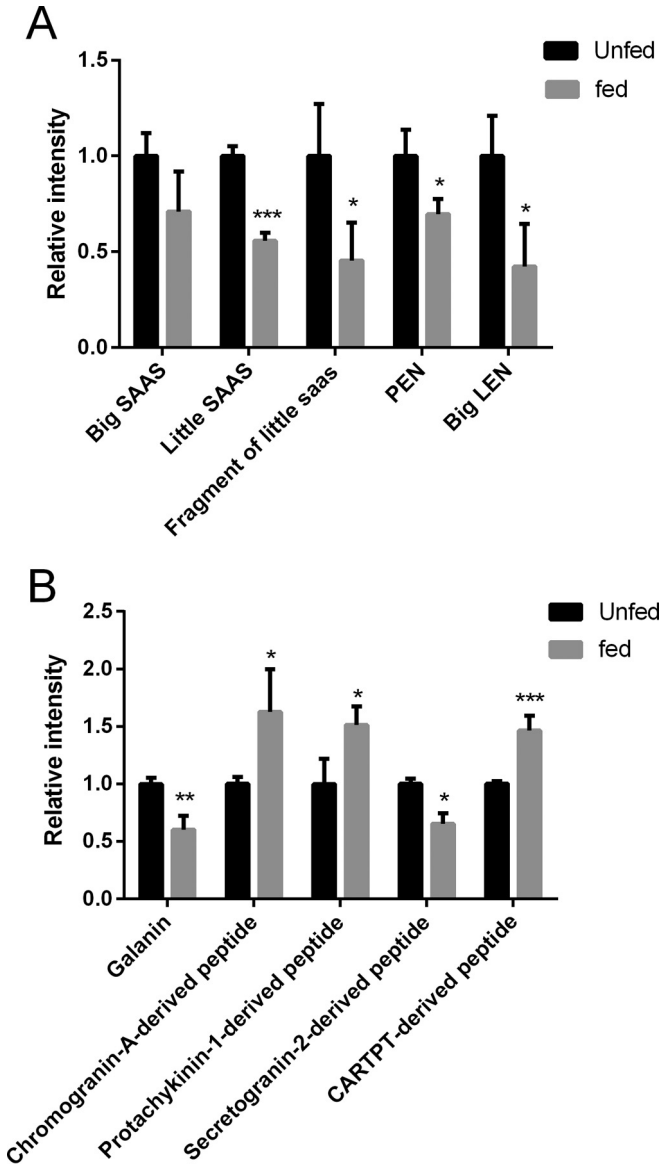

FIG. 4. **Label-free differential analysis of endogenous peptides in the nucleus accumbens (NAc).** *A*, Relative level changes of peptides derived from the ProSAAS precursor, including big SAAS, little SAAS, a truncated little SAAS (SLSAASAPLAETSTPL), PEN and big LEN. *B*, Relative level changes of galanin and linker peptides derived from chromogranin-A, protachykinin-1, secretogranin-2 and CART. Four tissue punches collected from NAcs of four individual rats were pooled as an aliquot for the quantitative analysis of peptidomic changes, and three aliquots were used for each group ($n = 3$). Values represent means ± S.E. * denotes $p < 0.05$, ** denotes $p < 0.01$, and *** denotes $p < 0.005$.

exhibited a significant decrease in the expression levels in rat NAc region on feeding. ProSAAS has long been associated with prenatal regulation of neuropeptide processing through regulation of prohormone convertases, whereas it has recently been revealed to possess alternative physiological functions in directly regulating body weight and other behaviors such as anxiety (39). As shown in Fig. 4*A*, we quantified several mature neuropeptides derived from the ProSAAS precursor, including big SAAS, ARPVKEPRSLSAASAPLAETSTPLRL; PEN, AVDQDLGPEVPPENVLGALLRV; big LEN, LENSSPQAPARRLLPP; little SAAS, SLSAASAPLAETSTPLRL and a truncated little SAAS, SLSAASAPLAETSTPL. Food intake downregulated these ProSAAS neuropeptides, despite a slightly varied degree of differences were displayed in their downregulation. For example, big LEN decreased ~58% ($p = 0.03$) and PEN decreased ~30% ($p = 0.03$). Little SAAS decreased ~44% ($p < 0.005$) and the truncated little SAAS decreased ~55% ($p = 0.048$). Other ProSAAS peptides detected from the NAc regions such as big SAAS also exhibited a downward trend on food intake, although the changes were not significant.

Beyond Pro-SAAS-derived peptides, we examined the feeding-dependent changes of other peptides derived from prohormones that are reported to be involved in the regulation of food intake and other physiological processes. As shown in Fig. 4*B*, differential analysis of galanin derived from the galanin peptide precursor, which has been implicated in the control of feeding (42, 43), showed a decrease of 40% in expression level after food intake, corroborating its putative functions as mediators that regulate food intake. In addition, by comparing the relative levels between the unfed and fed rats, we showed that the level of a secretogranin-2-derived peptide decreased by 35% ($p = 0.02$) after the food intake (see Table I).

We further compared the relative changes of several anorexigenic neuropeptide families. As in Fig. 4*B*, a truncated neuropeptide K derived from the protachykinin-1 precursor, DADSSIEKQVALLKALYGHGQISHK, was found to increase 51% ($p = 0.03$). Notably, a peptide fragment derived from the CART precursor also showed a significant increase of expression level by 41% ($p = 0.004$) after food intake compared with the unfed condition. Such changes agree with their previously reported functions as inhibitory regulators of feeding (44). Additionally, a chromogranin-A-derived peptide WSRMDQLAKELTAE exhibited an increase of 63% on feeding, suggesting its possible role involved in the regulation of food intake. A summary of all the other significantly changed peptides can be found in supplemental Table S4.

We then compared the relative expression levels of peptides among the NAc, HT, DS, and hippo. Intriguingly, some neuropeptides display different relative levels between NAc and other brain areas. For instance, as shown in supplemental Fig. S1, galanin and little SAAS were both significantly downregulated in NAc after feeding, yet remained constant in the HT of rat brain in response to food intake. In contrast, the expression level of GAV 1–25, AVPRGEAAGAVQELARALAHLLEAE, remained unchanged in the NAc on feeding, whereas it displayed a decrease of ~60% after the food intake in the HT region. The quantitative results of other peptides identified in different brain areas were summarized in supplemental Table S4.

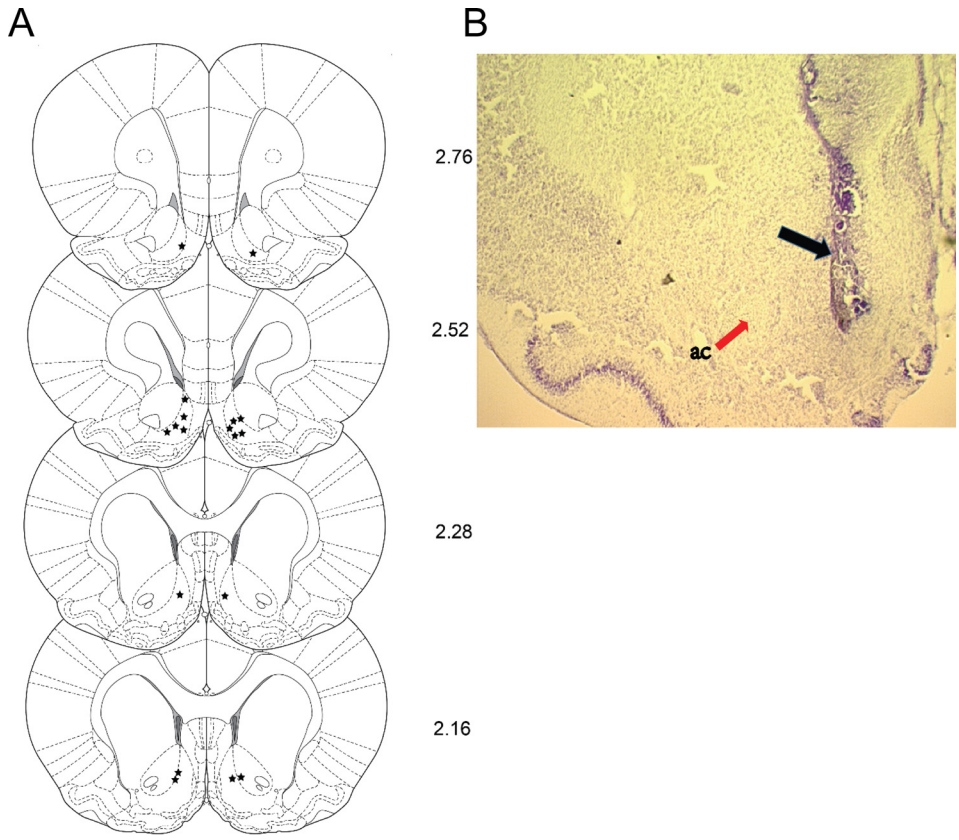

FIG. 5. **Injector placements for NAc shell-cannulated animals.** *A*, line drawings of coronal sections, depicting the injection sites from rats with bilateral placements in NAc where the position of each section from bregma was given in mm. Each injector tip placement is represented by a star symbol. *B*, photomicrographs showing injector placement into NAc shell, with black arrows indicating the location of injector tips. ac, anterior commissure (red arrow). Line drawing were adapted from the atlas of Paxinos and Watson (2007), with permission.

Microinjection of ProSAAS Peptides into Rat Nucleus Accumbens—Our label-free quantitative results have revealed several peptides derived from neuropeptide precursors exhibited expression level changes in response to fasting-induced food intake. Nevertheless, their functions in the NAc region have not yet been directly investigated. We selected the ProSAAS peptides as representative peptides whose expression levels changed significantly after food intake. We investigated their potential physiological functions in feeding regulation by microinjecting ProSAAS directly into the NAc, and measuring food and water ingestion and associated exploratory-like activity. Fig. 5 illustrates the histological verification of intra-NAc shell injection placements. Two rats were removed from the experiment because of guide cannulae obstruction or brain abscess. Fig. 5*B* shows representative photomicrographs of injector placements into the NAc shell; the injector tracks are clearly visible with no unusual damage to the area of interest.

The injector tips were found to be located within opioid-sensitive feeding zones; either the shell of NAc shell or the adjacent area between the shell and core. Fig. 5*A* depicts the schematic injector tip placement for each rat, whereas Fig. 5*B* illustrates the photomicrographs showing injector placement into NAc shell, with black arrow indicating the location of injector tips. ac, anterior commissure (red arrow).

A preliminary ANOVA on the three saline infusions conducted across the time-course of the experiment (*i.e.* pre-, mid-, and postpeptide saline infusions) did not reveal significant changes in food or water intake among these infusions (Ps $>$ 0.05). Therefore, for all intake and scored behavioral measures, these saline infusions were averaged together into one saline measure for use in the overall ANOVAs on peptide effects.

As shown in Fig. 6, DAMGO significantly elevated chow ($F(6, 7) = 18.291$, $p < 0.0001$) and water ($F(6, 7) = 7.024$, $p < 0.0001$) intake (see Fig. 6*A* and 6*B*). Posthoc comparison among means with Tukey-Kramer test confirmed that DAMGO-associated levels of food and water intake were significantly elevated relative to saline treatment. Although both doses (3, 10 μg) of PEN and big-LEN, and high dose of little-SAAS (10 μg) tended to increase mean food intake, only high dose (10 μg) of big-LEN achieved statistical significance ($F(5, 7) = 3.534$, $p = 0.0109$). Furthermore, the high dose (10 μg) of big-LEN elevated water intake in rats, relative to saline treatment ($F(5, 7) = 3.148$, $p = 0.0189$).

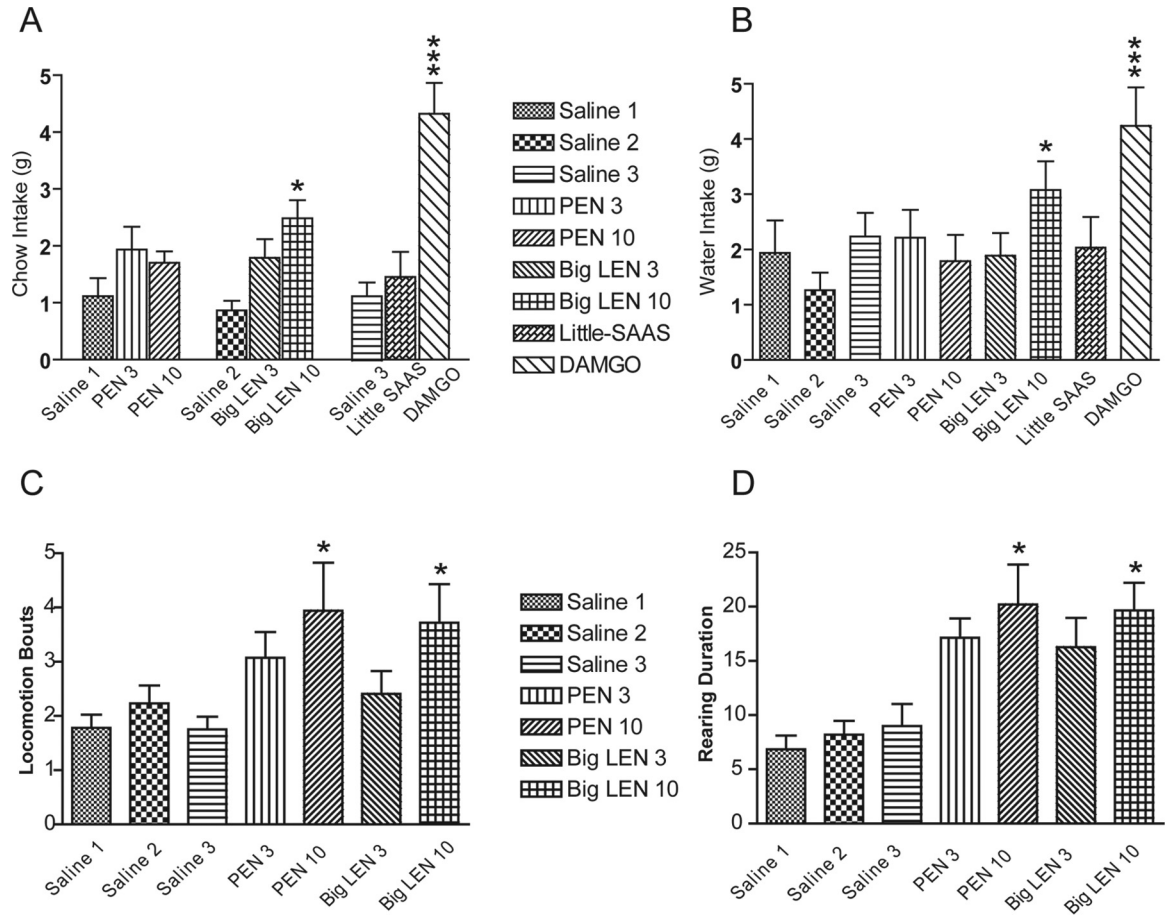

FIG. 6. **The effects of intranucleus accumbens shell infusions of ProSAAS-derived peptides in non-food-deprived rats (n = 8).** *A*, Alteration of chow intake in grams during two hour testing session with ProSAAS-derived peptides in comparison to saline and DAMGO. The high dose (10 μg/0.5 μl) of big-LEN significantly increased chow intake. *B*, Alteration of water intake during two-hour testing session with ProSAAS-derived peptides in comparison to saline and DAMGO. The high dose (10 μg/0.5 μl) of big-LEN produced a significant increase in water intake. *C*, Both the high dose of PEN and big-LEN (10 μg/0.5 μl for each peptide) significantly elevated locomotion in satiated rats compared with saline in the first hour. *D*, Both the high dose of PEN and big-LEN (10 μg/0.5 μl for each peptide) significantly increased the rearing duration in satiated rats compared with saline in the first hour. Values represent means ± S.E. * denotes $p < 0.05$, ** denotes $p < 0.01$, and *** denotes $p < 0.0001$.

For scored behavioral measures (*i.e.* locomotion, rearing, eating, drinking and grooming), there was a significant main effect of treatment for total locomotion ($F(4, 7) = 2.782$, $p = 0.0460$) and total duration of rearing bouts ($F(4, 7) = 3.688$, $p = 0.0156$) across the 60-min testing session. Furthermore, there were significant treatment × time interactions for locomotion ($F(66, 462) = 2.257$, $p < 0.001$) rearing bouts ($F(66, 462) = 2.578$, $p < 0.001$) and rearing duration ($F(66, 462) = 3.018$, $p < 0.001$), reflecting significant effects of PEN (10 μg) and LEN (10 μg) relative to saline treatment. No significant effects were seen with the lower (3 μg) dose of PEN or LEN. Time-course plots for locomotion and rearing are shown in Fig. 7.

DISCUSSION

The present quantitative neuropeptidome study combined cryostat dissection, heat stabilization, neuropeptide extraction, and label-free quantitative methodologies using a liquid chromatography-high resolution mass spectrometer to quantify endogenous peptides that displayed significant changes in response to food intake within specific regions of rat brain. Heat stabilization was performed efficiently and reproducibly via a tissue microwave irradiation device (Denator™) to curtail nonspecific protein degradation, thus enhancing the recovery of postmortem protein/peptide products. In addition, differential neuropeptide analyses were undertaken using a label-free method. The altered peptide abundance between unfed and fed groups were assessed using the precursor ions' intensities (based on chromatographically aligned spectra), which has been successfully applied to quantitative peptidome studies (29, 38, 45). This approach allows for direct monitoring of a wide dynamic range of peptides, and delivers a larger list of peptides that displayed altered expression levels compared with an isotopic labeling approach (46).

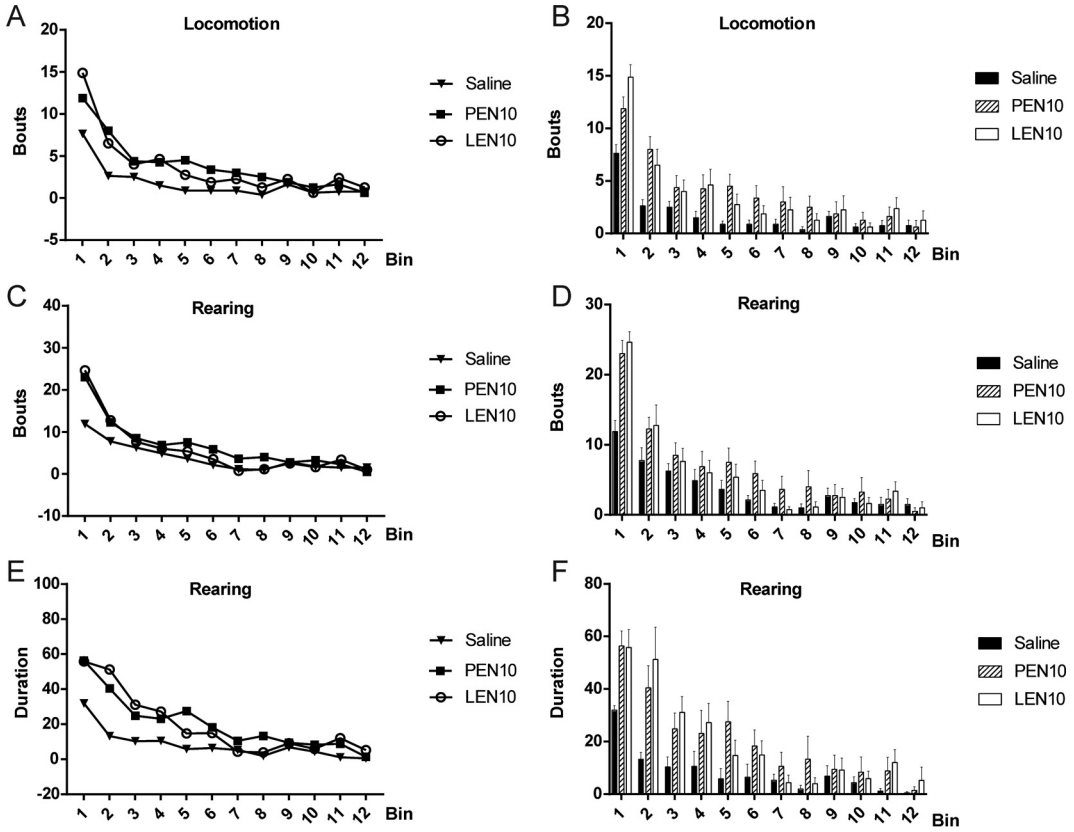

FIG. 7. **Time-course analysis of locomotion, rearing bouts and rearing duration during the first hour in rats.** (*A*), (*B*) Locomotion (P). (*C*), (*D*) Rearing bouts. (*E*), (*F*) Rearing duration ($p < 0.001$).

Our experimental paradigm has enabled us to comprehensively evaluate a multitude of neuropeptides involved in feeding from the NAc and other brain regions, including HT, DS and hippo. Although the changes of opioid peptides observed in this study are not statistically significant, likely because of larger individual variability and relatively small N number, we unveiled substantial changes of other peptides from families such as ProSAAS, galanin and CART in response to feeding in rat NAc. Furthermore, our study demonstrated behavioral actions of several ProSAAS peptides by intra-NAc microinjection experiments, suggesting the peptides discovered in the MS peptidomics approach might be physiologically relevant regulators of feeding behavior and thereby of great potential to be developed as molecular therapeutics.

In the present study, we exploited the natural circadian control of food intake to assess peptide dynamics in different feeding states, thereby approximating experimental conditions used in previous studies of feeding-related opioid peptide gene expression changes in the NAc (18). Rats forage for food at the beginning of the dark cycle (47). Hence, the animals were subjected to food deprivation at the beginning of the dark cycle—their natural time to eat. In this way, we sought to maximize the difference in motivational state, *i.e.* food-anticipatory *versus* satiated, to assess whether peptide levels are changed in response to food intake.

Intriguingly, we noted a pattern of flux (*i.e.* peptide levels higher in the food-anticipatory *versus* sated state) in peptides derived from the ProSAAS precursor peptide. Big SAAS, PEN, big LEN, and little SAAS detected in this study were bioactive end products of ProSAAS by sequential enzymatic processing. Big SAAS and PEN-LEN (not detected) are first produced from the precursor protein via initial cleavage by prohormone convertases. Consecutive processing further yields shortened peptides including little SAAS, PEN and big LEN (25). In contrast to a previous label-free quantitative study that showed different trends of big SAAS, PEN *versus* little SAAS, little PEN and big LEN in response to high fat/high sugar diet (38), our data sets exhibited a relatively uniform decrease of 40% within the NAc of fed group for big SAAS, PEN, big LEN, little SAAS, and a truncated little SAAS derived from the same precursor.

Previously, proSAAS has been considered as a neuropeptide precursor that functions by inhibiting prohormone convertase 1/3 (PC1/3). Recent studies (in transgenic mice overexpressing SAAS) have unveiled a broader role of this peptide family in influencing body weight and potentially inducing obesity and diabetes (48). For example, ProSAAS-derived peptides in HT were found to be elevated by food deprivation in $Cpe^{fat/fat}$ mice (49), suggesting its association to feeding. Moreover, ProSAAS-derived peptides were also shown to

colocalize with the feeding-regulatory peptide NPY in the mouse HT, and were concentrated in the arcuate nucleus (37). Because the receptors for several ProSAAS-derived peptides such as big LEN and PEN have been identified (50, 51), a small-molecule ligand of GPR171, a hypothalamic G protein-coupled receptor for Big LEN, was screened and demonstrated to increase food intake in mice through the activation of GPR171 (52). Taken together, these studies suggested the potential function of ProSAAS peptides as regulators of food intake. This was further corroborated by a study employing intracerebroventricular (icv) injections of antibodies to PEN, big LEN, little LEN, and little SAAS (37). Antibodies against PEN and big LEN exerted significant anorexigenic effects, whereas little LEN showed no effect on food intake and antibody to little SAAS exhibited a small increase of food intake. However, no significant effects on food intake were induced in mice injected with the ProSAAS-derived peptides to the HT region, possibly because of rapid degradation on icv injection in the mouse HT (37). In contrast, our findings provide direct evidence that ProSAAS-derived peptides can modulate feeding and associated behaviors at the level of the NAc, supporting the physiological roles of ProSAAS in the regulation of food intake. In line with these findings, ProSAAS-derived peptides might serve as future targets for therapeutic strategies in treating eating disorders.

At first glance, an increase of ProSAAS-derived peptides in the "unfed" (*i.e.* food-anticipatory) group might seem counterintuitive given that an agonist for the ProSAAS receptor increases feeding behavior. However, it is likely that ProSAAS-derived peptides are released on feeding and once released, are rapidly degraded. In the present experiment, we sacrificed our rats ~120 min after feeding; thus, the ProSAAS-derived peptides we extracted were likely from the secretory vesicles rather than the extracellular space. If this mechanistic assumption is considered, then the relative changes in ProSAAS-derived peptide expression levels fit within our working hypothesis: On eating, ProSAAS-derived peptides is released into the extracellular space where it is degraded. In contrast, rats anticipating food (but not having eaten yet) retain their pool of ProSAAS-derived peptides within the secretory vesicles (37); this ProSAAS-derived peptides store was detected with the mass spectrometry methods used in the present study.

As discussed above, peripheral administration of an agonist at hypothalamic receptor GPR171 (52), presumably a receptor for big LEN, induces feeding. However, to date, there has been no evidence of feeding-induced release of ProSAAS-derived peptides in the NAc. Here we employed a tissue punch approach to specifically collect the NAc region (see Fig. 1); hence, the above-mentioned increase of ProSAAS-derived peptides in the food-anticipatory state relative to the sated state reflected differential peptide levels within the NAc. As described above, one interpretation of these data is that ProSAAS-derived peptides build-up (in the food-anticipatory phase) within NAc-localized nerve terminals is released into the extracellular space during a meal, where it is rapidly degraded by peptidases. Note that this explanation does not preclude the simultaneous release of ProSAAS-derived peptides from the NAc into other areas of the brain; however, to our knowledge this is the first evidence (albeit indirect) of feeding-induced ProSAAS-derived peptides release within the NAc itself.

Similarly to ProSAAS-derived peptides, galanin was also significantly downregulated in the fed state. This observation is in accord with previous functional studies that has demonstrated stimulation of feeding by galanin (53, 54). In addition to ProSAAS-derived peptides and galanin, several truncated neuropeptides and linker peptides derived from prohormone precursors summarized in Table I showed significant expression level changes after feeding. These truncated and linker peptides are derived from precursors that have previously been implicated in the regulation of feeding behavior, such as protachykinin-1 and CART, or precursors that have not been clearly associated to feeding such as secretogranin-2 and chromogranin-A. Further biological studies are needed to elucidate their specific roles in regulation of food intake. Finally, another interesting finding in this study is that the peptides undergoing significant changes in NAc after feeding show different trends in other brain areas. Although the precise mechanism is unknown, such differences are likely because of tissue-specific processing and modulation of different neuropeptide precursors and their distinct regulatory roles in feeding within the NAc compared with other brain regions including HT, DS, or hippo.

CONCLUSIONS

In this study we report on the first characterization of the neuropeptidome of NAc in rat brain, with more than 300 peptides identified from this brain region. We further employed label-free quantitative mass spectrometry technique for differential analysis of NAc peptidome from fed and unfed rats. Our results revealed substantial expression level changes of multiple neuropeptides derived from different precursors, especially the ProSAAS-derived peptides and galanin. We further investigated potential functions of several ProSAAS-derived peptides by performing microinfusion experiments of these peptides to the NAc region of rat brain before and after feeding. We showed that big LEN significantly increased rats' food and water intake, whereas both big LEN and PEN affected other behaviors including locomotion, drinking and grooming. Collectively, our combined peptidomic analysis and behavioral study with selected peptides exhibiting altered expression patterns on feeding demonstrate peptide candidates that play important roles as regulators of feeding and associated behaviors, thus showing potential to be developed into molecular therapeutics for eating disorders in the future.

DATA AVAILABILITY

The mass spectrometric data have been deposited to the MassIVE system and accessible from ftp://massive.ucsd.edu/MSV000080106.

* This research was supported in part by NIH R01 DK071801. The Orbitrap instruments were purchased through the support of an NIH shared instrument grant (NIH-NCRR S10RR029531). LL acknowledges a Vilas Distinguished Achievement Professorship and a Janis Apinis Professorship with funding provided by the Wisconsin Alumni Research Foundation and University of Wisconsin-Madison School of Pharmacy.

[S] This article contains supplemental material.

§§ To whom correspondence should be addressed: School of Pharmacy and Department of Chemistry, University of Wisconsin–Madison, 777 Highland Avenue, Madison, WI 53705-2222. Fax: +1-608-262-5345; E-mail: lingjun.li@wisc.edu or Department of Psychiatry, University of Wisconsin-Madison School of Medicine and Public Health, 6001 Research Park Blvd, Madison, WI 53719. Fax: (608) 265-3050; Email: babaldo@wisc.edu.

¶¶ These authors contributed equally to this work.

REFERENCES

1. Schank, J. R., Ryabinin, A. E., Giardino, W. J., Ciccocioppo, R., and Heilig, M. (2012) Stress-related neuropeptides and addictive behaviors: beyond the usual suspects. *Neuron* **76,** 192–208
2. Podvin, S., Yaksh, T., and Hook, V. (2016) The Emerging Role of Spinal Dynorphin in Chronic Pain: A Therapeutic Perspective. *Annu. Rev. Pharmacol. Toxicol.* **56,** 511–533
3. An, S., Harang, R., Meeker, K., Granados-Fuentes, D., Tsai, C. A., Mazuski, C., Kim, J., Doyle F. J 3rd, Petzold, L. R., and Herzog, E. D. (2013) A neuropeptide speeds circadian entrainment by reducing intercellular synchrony. *Proc. Natl. Acad. Sci. U.S.A.* **110,** E4355–E4361
4. Navarro, V. M., and Kaiser, U. B. (2013) Metabolic influences on neuroendocrine regulation of reproduction. *Curr. Opin. Endocrinol. Diabetes Obes.* **20,** 335–341
5. Gautron, L., Elmquist, J. K., and Williams, K. W. (2015) Neural control of energy balance: translating circuits to therapies. *Cell* **161,** 133–145
6. Saper, C. B., Chou, T. C., and Elmquist, J. K. (2002) The need to feed: homeostatic and hedonic control of eating. *Neuron* **36,** 199–211
7. Spangler, R., Wittkowski, K. M., Goddard, N. L., Avena, N. M., Hoebel, B. G., and Leibowitz, S. F. (2004) Opiate-like effects of sugar on gene expression in reward areas of the rat brain. *Brain Res. Mol. Brain Res.* **124,** 134–142
8. DiLeone, R. J., Taylor, J. R., and Picciotto, M. R. (2012) The drive to eat: comparisons and distinctions between mechanisms of food reward and drug addiction. *Nat. Neurosci.* **15,** 1330–1335
9. Kelley, A. E., and Berridge, K. C. (2002) The neuroscience of natural rewards: relevance to addictive drugs. *J. Neurosci.* **22,** 3306–3311
10. Berridge, K. C. (2007) The debate over dopamine's role in reward: the case for incentive salience. *Psychopharmacology* **191,** 391–431
11. Pecina, S., and Berridge, K. C. (2000) Opioid site in nucleus accumbens shell mediates eating and hedonic 'liking' for food: map based on microinjection Fos plumes. *Brain Res.* **863,** 71–86
12. MacDonald, A. F., Billington, C. J., and Levine, A. S. (2004) Alterations in food intake by opioid and dopamine signaling pathways between the ventral tegmental area and the shell of the nucleus accumbens. *Brain Res.* **1018,** 78–85
13. Levine, A. S., and Billington, C. J. (2004) Opioids as agents of reward-related feeding: a consideration of the evidence. *Physiol. Behav.* **82,** 57–61
14. Zhang, M., and Kelley, A. E. (1997) Opiate agonists microinjected into the nucleus accumbens enhance sucrose drinking in rats. *Psychopharmacology* **132,** 350–360
15. Lord, J. A., Waterfield, A. A., Hughes, J., and Kosterlitz, H. W. (1977) Endogenous opioid peptides: multiple agonists and receptors. *Nature* **267,** 495–499
16. Pert, C. B., Pasternak, G., and Snyder, S. H. (1973) Opiate agonists and antagonists discriminated by receptor binding in brain. *Science* **182,** 1359–1361
17. Zhang, M., Gosnell, B. A., and Kelley, A. E. (1998) Intake of high-fat food is selectively enhanced by mu opioid receptor stimulation within the nucleus accumbens. *J. Pharmacol. Exp. Ther.* **285,** 908–914
18. Will, M. J., Vanderheyden, W. M., and Kelley, A. E. (2007) Striatal opioid peptide gene expression differentially tracks short-term satiety but does not vary with negative energy balance in a manner opposite to hypothalamic NPY. *Am. J. Physiol. Regul. Integr. Comp. Physiol.* **292,** R217–R226
19. van den Heuvel, J. K., Furman, K., Gumbs, M. C., Eggels, L., Opland, D. M., Land, B. B., Kolk, S. M., Narayanan, N. S., Fliers, E., Kalsbeek, A., DiLeone, R. J., and la Fleur, S. E. (2015) Neuropeptide Y activity in the nucleus accumbens modulates feeding behavior and neuronal activity. *Biol. Psychiatry* **77,** 633–641
20. Jureus, A., Cunningham, M. J., McClain, M. E., Clifton, D. K., and Steiner, R. A. (2000) Galanin-like peptide (GALP) is a target for regulation by leptin in the hypothalamus of the rat. *Endocrinology* **141,** 2703–2706
21. Griffond, B., and Risold, P. Y. (2009) MCH and feeding behavior-interaction with peptidic network. *Peptides* **30,** 2045–2051
22. Tachibana, T., Saito, S., Tomonaga, S., Takagi, T., Saito, E. S., Boswell, T., and Furuse, M. (2003) Intracerebroventricular injection of vasoactive intestinal peptide and pituitary adenylate cyclase-activating polypeptide inhibits feeding in chicks. *Neurosci. Lett.* **339,** 203–206
23. Hokfelt, T., Broberger, C., Xu, Z. Q., Sergeyev, V., Ubink, R., and Diez, M. (2000) Neuropeptides–an overview. *Neuropharmacology* **39,** 1337–1356
24. Buchberger, A., Yu, Q., and Li, L. (2015) Advances in Mass Spectrometric Tools for Probing Neuropeptides. *Annu. Rev. Anal. Chem.* **8,** 485–509
25. Fricker, L. D., McKinzie, A. A., Sun, J., Curran, E., Qian, Y., Yan, L., Patterson, S. D., Courchesne, P. L., Richards, B., Levin, N., Mzhavia, N., Devi, L. A., and Douglass, J. (2000) Identification and characterization of proSAAS, a granin-like neuroendocrine peptide precursor that inhibits prohormone processing. *J. Neurosci.* **20,** 639–648
26. Dowell, J. A., Heyden, W. V., and Li, L. (2006) Rat neuropeptidomics by LC-MS/MS and MALDI-FTMS: Enhanced dissection and extraction techniques coupled with 2D RP-RP HPLC. *J. Proteome Res.* **5,** 3368–3375
27. Svensson, M., Skold, K., Svenningsson, P., and Andren, P. E. (2003) Peptidomics-based discovery of novel neuropeptides. *J. Proteome Res.* **2,** 213–219
28. Che, F. Y., Lim, J., Pan, H., Biswas, R., and Fricker, L. D. (2005) Quantitative neuropeptidomics of microwave-irradiated mouse brain and pituitary. *Mol. Cell. Proteomics* **4,** 1391–1405
29. Petruzziello, F., Falasca, S., Andren, P. E., Rainer, G., and Zhang, X. (2013) Chronic nicotine treatment impacts the regulation of opioid and non-opioid peptides in the rat dorsal striatum. *Mol. Cell. Proteomics* **12,** 1553–1562
30. Sturm, R. M., Greer, T., Woodards, N., Gemperline, E., and Li, L. (2013) Mass spectrometric evaluation of neuropeptidomic profiles upon heat stabilization treatment of neuroendocrine tissues in crustaceans. *J. Proteome Res.* **12,** 743–752
31. Kelley, A. E., Baldo, B. A., and Pratt, W. E. (2005) A proposed hypothalamic-thalamic-striatal axis for the integration of energy balance, arousal, and food reward. *J. Comp. Neurol.* **493,** 72–85
32. Kanoski, S. E., and Grill, H. J. (2017) Hippocampus Contributions to Food Intake Control: Mnemonic, Neuroanatomical, and Endocrine Mechanisms. *Biol. Psychiatry* **81,** 748–756
33. Ye, H., Hui, L., Kellersberger, K., and Li, L. (2013) Mapping of neuropeptides in the crustacean stomatogastric nervous system by imaging mass spectrometry. *J. Am. Soc. Mass Spectrom.* **24,** 134–147
34. Zhang, J., Xin, L., Shan, B., Chen, W., Xie, M., Yuen, D., Zhang, W., Zhang, Z., Lajoie, G. A., and Ma, B. (2012) PEAKS DB: de novo sequencing assisted database search for sensitive and accurate peptide identification. *Mol. Cell. Proteomics* **11,** M111.010587
35. Kelley, V. B. A. (1991) Dopaminergic regulation of feeding behavior: I. Differential effects of haloperidol microinfusion into three striatal subregions. *Psychobiology* **19,** 9
36. Perry, M. L., Baldo, B. A., Andrzejewski, M. E., and Kelley, A. E. (2009) Muscarinic receptor antagonism causes a functional alteration in nucleus accumbens mu-opiate-mediated feeding behavior. *Behav. Brain Res.* **197,** 225–229

37. Wardman, J. H., Berezniuk, I., Di, S., Tasker, J. G., and Fricker, L. D. (2011) ProSAAS-derived peptides are colocalized with neuropeptide Y and function as neuropeptides in the regulation of food intake. *PLoS ONE* **6,** e28152
38. Frese, C. K., Boender, A. J., Mohammed, S., Heck, A. J., Adan, R. A., and Altelaar, A. F. (2013) Profiling of diet-induced neuropeptide changes in rat brain by quantitative mass spectrometry. *Anal. Chem.* **85,** 4594–4604
39. Morgan, D. J., Wei, S., Gomes, I., Czyzyk, T., Mzhavia, N., Pan, H., Devi, L. A., Fricker, L. D., and Pintar, J. E. (2010) The propeptide precursor proSAAS is involved in fetal neuropeptide processing and body weight regulation. *J. Neurochem.* **113,** 1275–1284
40. Hadjiconstantinou, M., and Neff, N. H. (2011) Nicotine and endogenous opioids: neurochemical and pharmacological evidence. *Neuropharmacology* **60,** 1209–1220
41. Bardo, M. T. (1998) Neuropharmacological mechanisms of drug reward: beyond dopamine in the nucleus accumbens. *Crit. Rev. Neurobiol.* **12,** 37–67
42. Crawley, J. N. (1999) The role of galanin in feeding behavior. *Neuropeptides* **33,** 369–375
43. Leibowitz, S. F. (2005) Regulation and effects of hypothalamic galanin: relation to dietary fat, alcohol ingestion, circulating lipids and energy homeostasis. *Neuropeptides* **39,** 327–332
44. Kristensen, P., Judge, M. E., Thim, L., Ribel, U., Christjansen, K. N., Wulff, B. S., Clausen, J. T., Jensen, P. B., Madsen, O. D., Vrang, N., Larsen, P. J., and Hastrup, S. (1998) Hypothalamic CART is a new anorectic peptide regulated by leptin. *Nature* **393,** 72–76
45. Lee, J. E., Zamdborg, L., Southey, B. R., Atkins, N., Jr, Mitchell, J. W., Li, M., Gillette, M. U., Kelleher, N. L., and Sweedler, J. V. (2013) Quantitative peptidomics for discovery of circadian-related peptides from the rat suprachiasmatic nucleus. *J. Proteome Res.* **12,** 585–593
46. Southey, B. R., Lee, J. E., Zamdborg, L., Atkins, N., Jr, Mitchell, J. W., Li, M., Gillette, M. U., Kelleher, N. L., and Sweedler, J. V. (2014) Comparing label-free quantitative peptidomics approaches to characterize diurnal variation of peptides in the rat suprachiasmatic nucleus. *Anal. Chem.* **86,** 443–452
47. Naber, D., Wirz-Justice, A., and Kafka, M. S. (1981) Circadian rhythm in rat brain opiate receptor. *Neurosci. Lett.* **21,** 45–50
48. Wei, S., Feng, Y., Che, F. Y., Pan, H., Mzhavia, N., Devi, L. A., McKinzie, A. A., Levin, N., Richards, W. G., and Fricker, L. D. (2004) Obesity and diabetes in transgenic mice expressing proSAAS. *J. Endocrinol.* **180,** 357–368
49. Che, F. Y., Yuan, Q., Kalinina, E., and Fricker, L. D. (2005) Peptidomics of $Cpe^{fat/fat}$ mouse hypothalamus: effect of food deprivation and exercise on peptide levels. *J. Biol. Chem.* **280,** 4451–4461
50. Gomes, I., Aryal, D. K., Wardman, J. H., Gupta, A., Gagnidze, K., Rodriguiz, R. M., Kumar, S., Wetsel, W. C., Pintar, J. E., Fricker, L. D., and Devi, L. A. (2013) GPR171 is a hypothalamic G protein-coupled receptor for BigLEN, a neuropeptide involved in feeding. *Proc. Natl. Acad. Sci. U.S.A.* **110,** 16211–16216
51. Gomes, I., Bobeck, E. N., Margolis, E. B., Gupta, A., Sierra, S., Fakira, A. K., Fujita, W., Muller, T. D., Muller, A., Tschop, M. H., Kleinau, G., Fricker, L. D., and Devi, L. A. (2016) Identification of GPR83 as the receptor for the neuroendocrine peptide PEN. *Sci. Signal.* **9,** ra43
52. Wardman, J. H., Gomes, I., Bobeck, E. N., Stockert, J. A., Kapoor, A., Bisignano, P., Gupta, A., Mezei, M., Kumar, S., Filizola, M., and Devi, L. A. (2016) Identification of a small-molecule ligand that activates the neuropeptide receptor GPR171 and increases food intake. *Sci. Signal.* **9,** ra55
53. de Pedro, N., Cespedes, M. V., Delgado, M. J., and Alonso-Bedate, M. (1995) The galanin-induced feeding stimulation is mediated via alpha 2-adrenergic receptors in goldfish. *Regul. Pept.* **57,** 77–84
54. Koegler, F. H., and Ritter, S. (1998) Galanin injection into the nucleus of the solitary tract stimulates feeding in rats with lesions of the paraventricular nucleus of the hypothalamus. *Physiol. Behav.* **63,** 521–527